CHAPTER SIX

CW-EPR Spectral Simulations: Solid State☆

Stefan Stoll[1]
Department of Chemistry, University of Washington, Seattle, Washington, USA
[1]Corresponding author: e-mail address: stst@uw.edu

Contents

Abstract

This chapter summarizes the core concepts underlying the simulation of EPR spectra from biological samples in the solid state, from a user perspective. The key choices and decisions that have to be made by a user when simulating an experimental EPR

☆This chapter is dedicated to Graeme Hanson (1955–2015), the creator of the EPR simulation program XSophe.

Methods in Enzymology, Volume 563
ISSN 0076-6879
http://dx.doi.org/10.1016/bs.mie.2015.06.003

spectrum are outlined. These include: the choice of the simulation model (the network of spins and the associated spin Hamiltonian), the dynamic regime (solid, liquid, slow motion), the level of theory used in the simulation (matrix diagonalization, perturbation theory, etc.), the treatment of orientational order and disorder (powder, crystal, partial ordering), the inclusion of the effects of structural disorder (strains), the effects of other line broadening mechanisms (unresolved hyperfine couplings, relaxation), and the inclusion of experimental distortions (field modulation, power saturation, filtering). Additionally, the salient aspects of utilizing least-squares fitting algorithms to aid the analysis of experimental spectra with the help of simulations are outlined. Although drawing from the experience gained from implementing EasySpin and from interacting with EasySpin's user base, this chapter applies to any EPR simulation software.

1. INTRODUCTION

In enzymology, biochemistry, and structural biophysics, solid-state EPR spectroscopy is used in two main contexts. First, it is used to study the structures of resting and intermediate states of radical enzymes, metalloenzymes, and metalloproteins which are constitutively paramagnetic (transition metal ions; metal ion clusters; protein-, substrate-, and cofactor-centered organic radicals). Second, solid-state EPR is used to determine conformations of proteins and protein complexes that are intrinsically diamagnetic, but are rendered paramagnetic by the site-selective introduction of spin labels.

The structure of the paramagnetic centers in these systems can be very rich and varied. As a consequence, they can give rise to a wide range of very diverse EPR spectra that often can only be analyzed with the help of computer simulations. Therefore, in addition to being familiar with published EPR spectra of the type of centers under study, a practitioner of EPR needs to be aware of the choices required in an EPR simulation. Improper choices can lead to erroneous conclusions, even if the simulations appear to be accurate and are perceived as correct.

In this overview, we review the concepts underlying the essential decisions that need to be taken when simulating and fitting EPR spectra. This provides a framework for performing robust EPR simulations, while minimizing the risk of making wrong conclusions from the data. This framework is general and independent of any particular simulation program. The author's program, EasySpin (Stoll & Schweiger, 2006), offers many choices on all aspects, whereas many other programs are more limited in scope (although just as correct within their scope, and often faster). The aspects discussed in this chapter are based on the experience gained from

implementing EasySpin and from interacting with its user base over the years, but are valid more generally.

This chapter will not discuss the theory underlying EPR simulations. For more details about that, see a recent comprehensive review on the subject (Stoll, 2014) that includes over 500 references. The general theory of solid-state EPR is laid out in several excellent textbooks and monographs (Abragam & Bleaney, 1986; Atherton, 1993; Bencini & Gatteschi, 1990; Mabbs & Collison, 1992; Pake & Estle, 1973; Pilbrow, 1990; Weil & Bolton, 2007).

The basic workflow for setting up an EPR simulation is as follows. First, an appropriate spin coupling network and an appropriate spin Hamiltonian (SH) model have to be chosen (Section 2). This is trivial for systems such as nitroxide radicals or copper complexes, but can be challenging if the molecular species giving rise to the EPR signal is not established. Second, the dynamical regime must be identified. This can be liquid, slow-motion, or rigid limit and depends on the rotational mobility of the paramagnetic center and potentially other dynamical processes. In this overview, we only discuss solid-state samples in the rigid-limit regime (Section 3). Third, an adequate and sufficiently accurate level of theory suitable to calculate EPR spectra from the given SH needs to be selected (Section 4). Most commonly, this is either matrix diagonalization or perturbation theory in combination with some sort of energy level diagram modeling. Fourth, knowledge of the orientational order or disorder of the sample is required (Section 5). This can be a powder, a crystal of a specific symmetry, or a partially ordered phase. Fifth, a decision has to be made as to how to model additional broadenings resulting from structural disorder, magnetic disorder, and relaxation processes (Sections 6 and 7). Sixth, it has to be ascertained that experimental effects due to saturation, field modulation, and filtering are properly accounted for (Section 8). Lastly, if the purpose of the simulation is to fit experimental data, then considerations about the type, scope, and utility of various least-squares fitting algorithms are important (Section 9).

2. SPINS AND SH

Most molecular paramagnetic systems can be simulated using a SH, which is an effective Hamiltonian that only depends on the spins of electrons and magnetic nuclei, and not their spatial coordinates. Effects of the crystal field and of spin–orbit coupling are folded into the parameters of this SH (Weil & Bolton, 2007).

The first decision to be made when setting up an EPR simulation is the number and types of electron and nuclear spins to include. Often, this is very obvious, especially for the electron spins. For example, for an organic radical, an electron spin of $S = 1/2$ is evident. On a single transition metal ion, all unpaired electrons are treated as a single total spin S. For example, for high-spin Fe(III) with five unpaired electrons, it would be $S = 5/2$. However, for multiple coupled paramagnets, this can be less obvious. In a cluster of metal ions, there are two possibilities. First, one can treat the spins on each ion explicitly and then include appropriate coupling terms into the SH. Second, if the coupling is sufficiently strong and only the lowest energy levels are observable by EPR, the entire metal ion cluster can be treated as a single total electron spin S_{tot}. For example, an antiferromagnetically coupled Fe(II)Fe(III) cluster can be modeled as a system with a Fe(II) with $S_1 = 2$ coupled to an Fe(III) with $S_2 = 5/2$, or as a single total spin with $S_{tot} = 1/2$. The choice between these uncoupled and coupled representations depends on the available experimental data and on the level of analysis that is desired (Bencini & Gatteschi, 1990).

The inclusion of nuclear spins also needs consideration. In a Cu(II) complex, one obviously must include the Cu nuclear spin. Sometimes, it is also necessary to include magnetic nuclei from the ligands. The decision of whether to include a magnetic nucleus explicitly in the SH depends on whether the effects from its hyperfine coupling to the electron spins are resolved or not. If they are resolved, the nucleus must be modeled explicitly. If they are not resolved, but only result in additional broadening, they should be treated as a line broadening mechanism (see Section 7).

Once the network of spins is chosen, the SH terms describing the interactions of the spins need to be chosen. SHs that allow accurate simulation of the EPR spectra from the great majority of paramagnetic systems contain only a few types of terms. These are listed in the following.

(A) Electron Zeeman interaction. For each electron spin in the system, a term of the form $\hat{H}_{EZI} = \mu_B \boldsymbol{B} g \hat{\boldsymbol{S}}$ must be included, with the Bohr magneton μ_B (in J/T), the magnetic field vector $\boldsymbol{B}$ (in T), and the spin vector operator $\hat{\boldsymbol{S}}$ (unitless). The 3×3 matrix, g, is called the g tensor or g matrix. For a free electron outside a molecular environment, it is diagonal and isotropic, with $g_e = 2.002319$ on the diagonal. In the presence of a molecular electrostatic environment it shifts from g_e. This g shift, $\Delta g = g - g_e$, is generally anisotropic in the sense that it depends on the orientation of the molecule with respect to the applied magnetic field. The g shift can be

interpreted in terms of molecular structural and electronic properties (Patchkovskii & Schreckenbach, 2004; Stoll, 2011).

(B) For each electron spin with spin >1/2, a zero-field splitting term is included in the SH. Its form is $\hat{H}_{\mathrm{ZFI}} = \hat{\boldsymbol{S}} D \hat{\boldsymbol{S}}$, with the 3×3 matrix D representing the zero-field interaction tensor, in energy units. The origin of these terms lies in the spin–spin interactions of the electrons constituting the spin >1/2, and in spin–orbit coupling (Neese, 2004). The zero-field interaction is often parameterized in terms of the scalar parameters D and E (Weil & Bolton, 2007). Typical values of D range from around $0.1\ \mathrm{cm}^{-1}$ for organic triplet radicals to $10\ \mathrm{cm}^{-1}$ and larger for high-spin transition metal centers.

(C) For electron spins with spin 3/2 and larger (e.g., in high-spin transition metal ions), it can be necessary to include higher-order zero-field terms proportional to $\hat{S}^4$ and $\hat{S}^6$ in the SH. There is a wide and confusing range of different conventions used for these terms (Rudowicz & Karbowiak, 2015). The predominant approach involves a linear combination of extended Stevens operators. For systems with cubic symmetry, the more traditional scalar parameters a and F are often employed instead (Abragam & Bleaney, 1986). The structural origin of these terms is usually the crystal field.

(D) For each pair of interacting electron spins, a coupling term has to be included in the SH. The most general form of this coupling is $\hat{H}_{\mathrm{ee}} = \hat{\boldsymbol{S}}_A J \hat{\boldsymbol{S}}_B$, with the 3×3 interaction matrix J, in energy units. The interaction can be broken down into three terms (Bencini & Gatteschi, 1990): (a) an isotropic term $J_0 \hat{\boldsymbol{S}}_A \hat{\boldsymbol{S}}_B$, often called the Heisenberg–Dirac–van Vleck (HDvV) Hamiltonian, with the isotropic exchange coupling constant J_0 (note that different conventions are used in the literature); (b) an antisymmetric exchange term written as $\boldsymbol{d}_{AB} \hat{\boldsymbol{S}}_A \times \hat{\boldsymbol{S}}_B$ with the parameter vector $\boldsymbol{d}_{AB}$ and called the Dzyaloshinskii–Moriya term; and (c) a dipolar term $\hat{\boldsymbol{S}}_A D_{AB} \hat{\boldsymbol{S}}_B$ with the traceless 3×3 matrix D_{AB} describing dipolar interactions. Very often, the isotropic component dominates, and the other two terms are neglected.

(E) Beyond these standard SH terms for the electron spins, there are others with much rarer occurrence. These terms include biquadratic exchange $-j\left(\hat{\boldsymbol{S}}_A \hat{\boldsymbol{S}}_B\right)^2$ (Harris & Owen, 1963) and high-order Zeeman terms of dimension $B\hat{S}^3$ and $B\hat{S}^5$ (Claridge, Tennant, & McGavin, 1997). Very

few simulation programs implement them explicitly (Mombourquette, Tennant, & Weil, 1986).

(F) For each pair of nuclear spin and electron spin, a hyperfine coupling term is included in the SH. Its form is $\hat{H}_{\mathrm{HFI}} = \hat{\boldsymbol{S}}A\hat{\boldsymbol{I}}$, with the 3×3 hyperfine matrix A, in energy units, and the nuclear spin vector operator $\hat{\boldsymbol{I}}$ (unitless). The hyperfine interaction can be decomposed into three terms of different physical origin: (a) the isotropic Fermi contact term $A_0\hat{\boldsymbol{S}}\hat{\boldsymbol{I}}$, (b) the through-space spin-dipolar coupling term $\hat{\boldsymbol{S}}A_{\mathrm{dip}}\hat{\boldsymbol{I}}$ with the traceless matrix A_{dip}, and (c) the spin–orbit term $\hat{\boldsymbol{S}}A_{\mathrm{orb}}\hat{\boldsymbol{I}}$ with the 3×3 coupling matrix A_{orb}. This last term can be neglected in organic radicals, but must be taken into account in transition metals with large spin–orbit coupling (i.e., large g shifts).

(G) For each nuclear spin that is included in the SH model, there is a nuclear Zeeman term of the form $\hat{H}_{\mathrm{NZI}} = -\mu_{\mathrm{N}}g_{\mathrm{n}}\boldsymbol{B}\hat{\boldsymbol{I}}$, with the nuclear magneton μ_{N} (in J/T) and the nuclear g factor g_{n} (unitless), which is an isotope-specific constant that ranges from about −4 to +6. In molecular environments, g_{n} is slightly shifted from its free atom value and is anisotropic. This chemical shift anisotropy is in the ppm range and is too small to be resolved in EPR experiments. Therefore, it is always neglected and omitted from the SH.

(H) Finally, for each nuclear spin with spin >1/2, a nuclear quadrupole term of the form $\hat{H}_{\mathrm{NQI}} = \hat{\boldsymbol{I}}Q\hat{\boldsymbol{I}}$ is present in the SH. Q is the 3×3 matrix that describes the interaction of the nuclear electric quadrupole moment with the local electric field gradient. Effects of this term can occasionally be observed in CW-EPR spectra of 5d transition metals ions (Shaw et al., 2006). For CW-EPR of biologically abundant first-row transition metal ions and for organic radicals, this term can be generally neglected. In these cases, pulse EPR can be used to resolve this term.

(I) Lastly, there exists nuclear spin–spin coupling between each pair of magnetic nuclei in a molecule, both through-space and through-bond. Since the energies of these interactions are very low, they are not resolvable by EPR and are neglected in EPR simulations.

The SH terms listed above rely on the assumption that the electronic ground state observed by EPR is orbitally nondegenerate and that spin–orbit coupling is weak enough that it can be treated using second-order perturbation theory. When the ground state is orbitally degenerate, or the spin–orbit coupling is substantial, the explicit inclusion of orbital angular momentum effects is necessary. This can be achieved by going beyond the SH

approximation and introducing into the Hamiltonian terms that depend on orbital angular momentum operators. Either effective terms or first-principles terms can be used. Such terms are implemented in several programs for the simulation of magnetometry data (Borrás-Almenar, Clemente-Juan, Coronado, & Tsukerblat, 2001; Chilton, Anderson, Turner, Soncini, & Murray, 2013; Speldrich, Schilder, Lueken, & Kogerler, 2011), but presently not available in common EPR simulation programs.

3. DYNAMIC REGIME

With spins and SH chosen, the dynamic regime of the sample has to be identified. The dynamic regime will determine other simulation choices, such as the level of theory.

The timescale of all microscopic dynamic processes affecting the paramagnetic center and its SH need to be determined and compared to the appropriate timescale of the EPR experiment. Three cases are distinguished: (a) If a dynamic process is much faster than the EPR timescale, then its effect on the EPR spectrum is averaged, and the description can be simplified by averaging the modulation of the SH occurring over time. This is called the fast-motion regime. (b) If a dynamic process is on a timescale comparable to the EPR timescale, it will have a profound effect on the EPR spectrum and needs to be modeled explicitly. This is the slow-motion regime. (c) If a dynamic process is much slower than the EPR timescale, then the paramagnetic centers appear to be static for EPR purposes. To simulate an EPR spectrum in this rigid-limit regime, an explicit average over all quasi-static configurations resulting from the dynamic process has to be calculated.

The most common dynamic process in EPR is rotational diffusion, the tumbling of paramagnetic centers in a liquid environment. The timescale of this process is characterized by the rotational correlation time, τ_c. If τ_c is much shorter than the inverse of the spectral width of the EPR powder spectrum in angular frequency units, $\Delta\omega$, then the system is in the fast-motion regime, all the anisotropic interactions in the SH are averaged out, and the isotropic part of the SH is sufficient for an accurate simulation. If τ_c is much longer than $\Delta\omega^{-1}$, then the full SH is required. For a nitroxide radical at 0.35 T, the spectral spread is on the order of $\Delta\omega \approx 2\pi \cdot 180\text{MHz}$, so the EPR timescale is $\Delta\omega^{-1} \approx 0.9\text{ns}$.

Besides rotational diffusion, there are potentially other dynamical processes present. These include equilibria between several conformational

or oxidation states, proton transfers, or methyl group rotations (Hudson & Luckhurst, 1969). These cases are called chemical exchange and need to be modeled explicitly if their timescale is comparable to the timescale of the EPR experiment. Due to the variety of possible situations, chemical exchange simulation software is available only for specific systems (Heinzer, 1971; Zalibera et al., 2013).

In this chapter, we limit the discussion to the rigid limit, i.e., to systems that are rotationally frozen and do not undergo any other dynamical process. This is the case for frozen aqueous solutions of paramagnetic centers, powders, and glasses (e.g., proteins immobilized at room temperature by embedding into, or attachment onto, a solid matrix). The treatment of the effect of rotational diffusion on the EPR spectra of nitroxides is discussed expertly in "CW-EPR Spectral Simulations: Slow-Motion Regime" by David Budil in this volume.

Notice that the fast-motion limit of rotational diffusion can be treated within the same framework as the rigid limit. In the fast-motion limit, the dynamical process produces an isotropic Hamiltonian, but does otherwise not affect the EPR spectrum. Any level of theory used for the rigid limit can therefore be used to simulate fast-motion limit EPR spectra.

4. LEVELS OF THEORY

In the rigid limit, various levels of theory can be utilized to simulate a field-swept EPR spectrum. They include brute-force field sweeps, eigenfields, matrix diagonalization, and perturbation theory, in order of decreasing generality, but increasing speed.

EPR spectra are acquired as field sweeps, where the microwave frequency is kept constant and the magnetic field is swept over a specified range. Typically, the simulation of field sweeps occurs in two steps: (a) the energy eigenvalues and possible eigenstates are determined for one or several field values in the sweep range and (b) these data are used to determine the actual resonance fields.

4.1 Calculation of Energy Levels

For a given SH and a given value of the external magnetic field, the energies and eigenstates can be calculated either by diagonalization or perturbation theory, or a combination thereof.

(A) SH diagonalization is the general method. The SH is expressed as a $N \times N$ matrix in a basis of spin states, commonly the Zeeman product states. N is the number of spin states in the system. Diagonalization can

be applied to any SH and yields results that are exact within numerical accuracy. Since the computational time required for diagonalization scales as N^3, diagonalization can be very slow for large spin systems. Two common cases of large systems include organic radicals with many nuclei coupled to the electron spin, and coupled clusters of transition metal ions. In these cases, it is usually possible to resort to more approximate techniques. If only a small subset of the energy levels is accessible in the EPR experiments, subspace methods such as Davidson diagonalization can be used (Piligkos et al., 2009).

(B) Perturbation theory is the principal alternative to SH diagonalization. It can be used for organic radicals and for transition metal ions with small hyperfine couplings or small zero-field splittings. This applies to cases where the electron Zeeman interaction is much larger than any other SH term. First, energy levels due to the electron Zeeman interaction are calculated analytically. The effect of all hyperfine interactions, and of the zero-field interaction for $S > 1/2$, is then added as a perturbation (Iwasaki, 1974). Perturbation theory can be applied to systems with dozens of nuclei. First-order and second-order perturbation theory are most common, with the latter significantly more accurate than the former. Many programs implement some form of perturbation theory, but they rarely check whether the approach is valid. It is best to use second-order perturbation theory, but limit its use to cases where the electron Zeeman interaction is at least 20 times larger than any other interaction in the SH. Most perturbation theory is applied to systems with a single electron spin, although it can also be applied to systems of coupled electron spins with weak couplings.

(C) Hybrid methods are available in cases of multiple strongly coupled electron spins with additional hyperfine couplings. Hybrid methods work in two steps. First, the system of coupled electron spins without the nuclear spins is treated exactly via matrix diagonalization. Then, the effect of hyperfine coupling to the nuclei is included perturbationally. This method is valuable for systems such as manganese clusters (Golombek & Hendrich, 2003).

4.2 Energy Level Diagram Modeling

The next step in the simulation of an EPR spectrum is the determination of the resonance fields, i.e., those field values where the microwave photon energy $h\nu_{\mathrm{mw}}$ matches an energy difference between two energy levels,

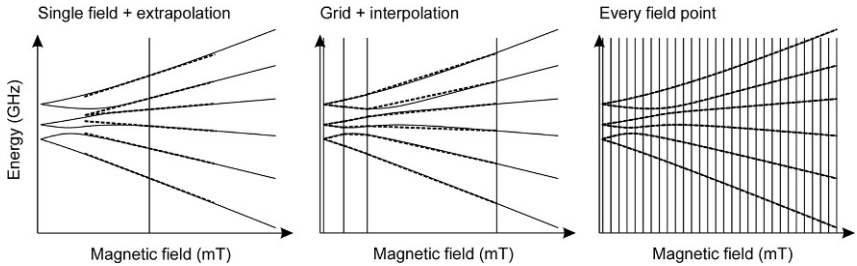

Figure 1 Different approaches to energy level diagram modeling. Left: Calculation at a single field value combined with extrapolation. Center: Calculation at a few grid points combined with interpolation. Right: Calculation at every single field value.

$h\nu_{\mathrm{mw}} = E_b(B) - E_a(B)$. For this, the energy level diagram $E(B)$ (energy vs. field) has to be calculated.

There are three ways of doing that, illustrated in Fig. 1. (1) If resonances are expected only within a narrow field range, then it is often sufficient to extrapolate from energy level values and slopes at a single field value such as the center field B_0 of the sweep range. This works well for organic radicals, but can be very wrong for any other system. (2) If the spectrum is broader, then a larger field range has to be modeled. This can be done by calculating energy values and states at a specific set of field values, either on a predefined grid (Wang & Hanson, 1995) or on a grid that adapts itself to the complexity of the energy level diagram (Stoll & Schweiger, 2003). Resonance fields are then determined by interpolation between these grid points. (3) If the energy level diagram is very complicated and contains a lot of avoided crossings, interpolation can potentially fail. In this case, the brute-force method of calculating $E(B)$ at every field value over the field range is the safe fallback method.

4.3 Eigenfields

The eigenfield method is the single method that does not rely on modeling the energy level diagram for the computation of resonance fields (Belford, Belford, & Burkhalter, 1973). It directly calculates resonance fields from the SH within numerical accuracy. To achieve this, the SH is represented as a "supermatrix" in Liouville space that includes the microwave frequency. This matrix is of size $N^2 \times N^2$ and is diagonalized, directly yielding the resonance fields as eigenvalues (eigenfields). Due to the large matrix dimensions involved, the eigenfields approach is impractically slow for simulations of

any but the smallest spin systems. However, it is exceptionally useful as a reference method, primarily for systems with many energy levels involving anticrossings, where resonance fields can span a wide field range.

5. ORIENTATIONAL ORDER AND DISORDER

When simulating the EPR spectrum of a solid-state sample, the orientational probability distribution $P(\boldsymbol{\Omega})$ of the paramagnetic centers present within the sample needs to be taken into account. $\boldsymbol{\Omega}$ indicates a set of three Euler angles (ϕ,θ,χ) that describe the orientation of a paramagnetic center relative to the laboratory. The two limiting situations are crystals, where only a few discrete orientations are present ($P(\boldsymbol{\Omega}) = \delta(\boldsymbol{\Omega} - \boldsymbol{\Omega}_k)/n_s$ for $k = 1 \ldots n_s$), and powders, where all possible orientations of the paramagnetic center occur with equal probability, $P(\boldsymbol{\Omega}) = 1/8\pi^2$. Between these two extremes, there are partially ordered systems, such as aligned membranes or powders with crystallites that align in the field.

5.1 Crystals

The EPR spectrum of a single crystal depends on the symmetry of the crystal, specified by its space group. A single crystal is made of a regular translational repetition of a unit cell. A unit cell in turn is a combination of one or more asymmetric units. All asymmetric units in the unit cell can be generated from a single one using the symmetry operations of the space group of the crystal. Typically, there is one paramagnetic center per asymmetric unit. As a result, there will be several paramagnetic sites per unit cell (site multiplicity n_s), with potentially different orientations and therefore different EPR spectral signatures.

The site multiplicity depends on the space group symmetry. EPR spectroscopy is not sensitive to translations, that is, the spectrum of a paramagnetic center does not depend on where it is located in the EPR sample. Therefore, all the translational symmetries in crystals are irrelevant in EPR and can be neglected. Additionally, all EPR spectra are inversion symmetric, that is, if all the atom positions in a crystal are inverted across a fixed point in space (the inversion center), the EPR spectrum does not change. As a consequence, only the rotational characteristics of the space group are relevant to EPR. Based on that, the 230 space groups fall into 11 groups, called Laue groups (Weil, Buch, & Clapp, 1973). All crystals in the same Laue group have identical site multiplicity, which ranges from 1 to 24.

For the EPR simulation of single crystals, it is crucial to accurately describe the orientation of magnetic tensors within the paramagnetic center, the orientation of paramagnetic centers within the crystal, and the orientation of the crystal with respect to the laboratory. The relative orientations between each pair of frames are described by sets of three Euler angles. Each simulation program has its own conventions for the definition of the various molecule- and laboratory-fixed coordinate frames. Care has to be exercised to adhere to these conventions, and also to document them meticulously in a publication.

5.2 Powders

In powders and frozen solutions, any orientation of the paramagnetic center occurs with equal probability. The line positions in the EPR spectrum depend on the first two of the three Euler angles $\boldsymbol{\Omega} = (\phi, \theta, \chi)$ that describe the relative orientation between the center and the laboratory frame. The third angle χ affects the line intensities only and can be treated analytically. For the integration over the first two Euler angles ϕ and θ, summation over a discrete grid is necessary except for the simplest $S = 1/2$ systems (Kneubühl, 1960).

Grids over (ϕ, θ) can be represented as a set of points on the unit sphere. There is a host of (ϕ, θ) grids that have been developed over many years (Ponti, 1999). Simulation programs often differ in the type of grid they use. In EPR, triangular grids such as the SOPHE grid (Wang & Hanson, 1995) and the EasySpin grid (Stoll & Schweiger, 2006) are common, but spiral grids (Pilbrow, 1990) and Lebedev grids (Stevensson & Edén, 2006) have been used as well. A typical grid is shown in Fig. 2.

For each grid point, the single-orientation spectrum is calculated, and at the end, all spectra are combined to give the powder spectrum. The smoothness of the final powder spectrum depends on the grid resolution, which is determined by the user. If the resolution is too coarse, the spectrum will show discretization noise. The grid resolution required depends on the overall width of the powder spectrum: The wider the spectrum, the higher the required grid resolution.

Some programs go beyond the simple sum-all-grid-points method and generate more single-orientation data by interpolating line positions and intensities between two adjacent grid points or by calculating the partial powder spectrum due to a small region on the (ϕ, θ) plane. These advanced methods result in substantial gains in the speed and smoothness of powder simulations (Stoll & Schweiger, 2006; Wang & Hanson, 1995).

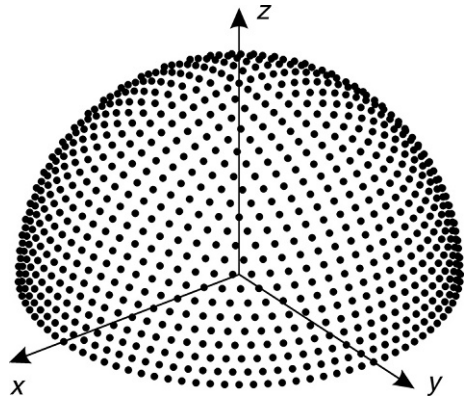

Figure 2 A typical spherical (ϕ,θ) grid used in EPR powder simulations (SOPHE grid with $N = 25$). The dots indicate the grid points in polar coordinates corresponding to (ϕ,θ). Due to the inversion symmetry of EPR spectra, only one hemisphere is needed.

The most challenging aspect of powder simulations are looping transitions. These are orientation-dependent transitions between two energy levels, E_a and E_b, that occur at two fields for a subset of orientations, but vanish for another subset of orientations because the microwave photon energy is not able to bridge the energy gap for any field within the sweep range. At the border between these two sets of orientations, the two resonance lines coalesce in the field sweep and then vanish. Simulation of looping transitions is challenging because the resonance fields are extremely sensitive to the orientation of the paramagnetic center in the sense that a small angle change in ϕ or θ leads to a large change in the line position. Spherical grids with very high resolution are required in order to get smooth spectra without artifact features near the coalescence points. Alternatively, dedicated methods for looping transitions can be used (Gaffney & Silverstone, 1998). Looping transitions occur in high-spin systems with zero-field splittings that are on the order of the microwave photon energy.

5.3 Partially Ordered Samples

In samples such as biological membranes, aligned films, or magnetically aligned powders, the orientational distribution $P(\boldsymbol{\Omega})$ of spin centers may deviate from uniform random, as the spin centers can have preferential alignment along a specific direction or in a specific plane. A nonuniform $P(\boldsymbol{\Omega})$ is often described using an ordering potential $U(\boldsymbol{\Omega})$, via $P(\boldsymbol{\Omega}) \propto \exp(-U(\boldsymbol{\Omega})/k_{\mathrm{B}}T)$ with the Boltzmann constant k_{B} and the temperature T. Partial ordering is included in a powder simulation by weighing the contributions from each spherical grid point according to $P(\boldsymbol{\Omega})$.

Orientational distributions based on an ordering potential are extensively used in the simulation of tumbling paramagnets such as nitroxides using the stochastic Liouville equation (see "CW-EPR Spectral Simulations: Slow-motion Regime" by David Budil in this volume). When $U(\boldsymbol{\Omega})$ is fitted to spectral data, it is commonly expanded in a linear combination of a few basis functions such as spherical harmonics $Y_M^L(\phi,\theta)$ or Wigner functions $D_{MK}^L(\phi,\theta,\chi)$ with low orders L. A high-accuracy determination of the orientational order from experimental EPR spectra beyond these lowest orders is generally not possible.

6. STRUCTURAL ORDER AND DISORDER

In addition to orientational disorder, the potential presence of structural disorder also needs to be taken into account in EPR simulations. In a solid-state sample, the structure of most paramagnetic centers can vary from site to site. In glasses and frozen solutions, the amorphous molecular environment surrounding the paramagnetic center induces structural distortions in the paramagnetic centers that vary from site to site. Even in crystals, small site-to-site variations in the geometry are possible. Since molecular structure determines the SH parameters, a consequence of this site-to-site structural variability is that SH parameters do not have unique values, but are distributed. If we label the affected SH parameters as p_i, then this means the distribution $P(p_1,p_2,p_3,\ldots)$ has nonzero width. Such distributions are called strains. Distributions in g values are termed g strain, distributions in hyperfine values are called A strain, and distributions in zero-field splitting parameters are called D strains or D/E strains.

There are two ways to take $P(p_1,p_2,p_3,\ldots)$ into account in a simulation. First, the simple way is to assume that the distribution is Gaussian along each parameter and that the distribution is narrow compared to the average value of the parameter. For example, a Gaussian hyperfine distribution with a mean of 100 MHz and a standard deviation of 5 MHz would fulfill this requirement. In this case, the dependence of the EPR resonance field position on each SH parameter can be approximated as linear (using the Hellmann–Feynman theorem), and the effect of the strain can be treated as simple additional line broadening. This method is usually sufficient for g distributions in high-field EPR spectra of organic radicals and in standard EPR spectra of iron complexes (Hagen, Hearshen, Sands, & Dunham, 1985). Correlated distributions of g and A in Cu(II) complexes can be treated as well (Froncisz & Hyde, 1980). Correlated distributions in the zero-field

splitting parameters D and E are used for high-spin systems (Hagen, 2007; Weisser, Nilges, Sever, & Wilker, 2006).

The second way is more exact but much more expensive: choose an explicit distribution $P(p_1, p_2, p_3, \ldots)$ of the SH parameters, set up a grid in this parameter space, explicitly loop over all the grid points, calculate the corresponding EPR spectra, and then average them using distribution values as weights. With this, it is possible to quantitatively treat non-Gaussian distributions and distributions that are very wide. Also, this explicit treatment can easily take into account correlation between any pair of SH parameters. This approach is required for modeling the wide distributions of zero-field splitting parameters that occur in high-spin transition metal complexes. Often, the simulated spectrum is not very sensitive to the exact distribution model if the distribution is very wide. Explicit numerical integration over a grid is of course much more costly in terms of computational time.

7. OTHER LINE BROADENINGS

Beyond orientational and structural disorder, there are several other potential sources of broadening. Prior to running a simulation, it must be assessed whether these mechanisms are relevant or not. If they are, they need to be modeled.

The most common additional source of broadening is due to magnetic disorder, the site-to-site variation of the magnetic environment even for sites that are structurally identical. One major source is unresolved hyperfine couplings to surrounding magnetic nuclei that are not explicitly included in the SH model. This broadening is typically approximated as Gaussian in shape and its width is very often anisotropic.

Commonly, the concentration of paramagnetic centers in an EPR sample is such that it is magnetically dilute, i.e., adjacent paramagnetic centers are far enough away from each other so that the dipolar through-space magnetic coupling between them is negligible compared to the smallest intra-center interaction. In concentrated samples, this might not be the case, and significant inter-center coupling can lead to additional broadening in the EPR spectrum. In solid-state EPR spectra of proteins with the paramagnetic centers buried in active sites, this is rarely a problem. However, it can be a problem when studying highly concentrated small-molecule-based paramagnetic centers. Also, it can occur in a frozen solution if the paramagnetic centers aggregate during the freezing process.

Another potentially important source of broadening in solid-state EPR is spin relaxation. An EPR transition with a transverse relaxation time constant of T_2 gives rise to a Lorentzian line with a width of $T_2^{-1}/2\pi$ in the frequency domain and of T_2^{-1}/γ_e in the field domain, where γ_e is the gyromagnetic ratio of the electron spin. This additional Lorentzian broadening needs to be modeled if it is not negligible compared to the other sources of broadening, i.e., when T_2 is short and the transverse relaxation rate is fast.

8. EXPERIMENTAL EFFECTS

The nature of the measurement process in standard CW-EPR can impart certain distortions onto the EPR spectrum. If these distortions are not avoided during the acquisition of the experimental spectrum, they must be explicitly included in the simulation. Below, we mention field modulation, saturation, and filtering. Additionally, misalignment of the microwave phase can lead to absorption/dispersion admixture that needs to be taken into account as well.

8.1 Field Modulation

Continuous-wave EPR uses field modulation combined with phase-sensitive detection to obtain spectra with good sensitivity. Simulation programs initially simulate the absorption spectrum without field modulation. In a second step, the effect of field modulation is then included at one of the three levels of increasing complexity and generality. (1) If the modulation amplitude is small relative to the narrowest spectral feature, then it is sufficient to approximate the effect of the field modulation by taking the derivative of the absorption spectrum with respect to the magnetic field. (2) The second level of treatment is based on a digital filter in the field domain. In this approach, the absorption spectrum is convoluted with a lineshape that approximately represents the effect of the modulation, including overmodulation if the modulation amplitude is larger than the narrowest spectral feature. This approach allows the accurate simulation of overmodulated spectra (Hyde, Pasenkiewicz-Gierula, Jesmanowicz, & Antholine, 1990; Nielsen, Hustedt, Beth, & Robinson, 2004). (3) Third, the effect of the field modulation can be taken into account in a full quantitative way that includes both modulation amplitude and frequency. This entails determining steady-state solutions of the underlying equations of motions (Bloch equations, Liouville–von Neumann equation) and is more time-intensive than the other two methods (Robinson, Mailer, & Reese, 1999). The main benefit

of this approach is that it can accurately model the appearance of modulation side bands. These occur when the modulation frequency is larger than the inverse linewidth of an EPR absorption line. In practice, this situation hardly ever occurs in biological EPR, since the lines are generally broad compared to the standard range of modulation frequencies (up to 100 kHz).

8.2 Saturation

If the microwave power in the experiment is too large, such that the saturation factor $1/\left(1+\gamma_e^2 B_1^2 T_1 T_2\right)$ significantly deviates from 1, then the EPR spectrum is partially saturated and the lines are broadened. B_1 is the strength of the magnetic component of the microwave at the sample. In this case, the EPR spectrum is broadened and weakened by an additional factor of $\sqrt{1+\gamma_e^2 B_1^2 T_1 T_2}$. Since the longitudinal and transverse relaxation times, T_1 and T_2, can be orientation dependent, saturation can lead to orientation-dependent Lorentzian broadening. Generally, it is best to avoid this situation experimentally by choosing a sufficiently low microwave power so that an unsaturated spectrum is recorded.

8.3 RC Filtering

Many EPR spectrometers have a setting that allows smoothing of the spectral data while they are acquired. Typically, a hardware RC filter is used. The user adjusts the time constant of the RC filter to reduce the noise in the acquired spectrum. If the time constant is too large, the spectrum is oversmoothed and spectral detail can be lost. Therefore, it is strongly recommended not to use built-in RC filters and perform all necessary smoothing digitally on the acquired data. Digital postprocessing is preferable, since it is nondestructive. Nevertheless, if RC filtering was used to acquire EPR data, it needs to be taken into account in the simulation, especially if an accurate analysis of the experimental lineshapes is of interest. Digitally, an RC filter can be applied to a simulated spectrum using a simple convolution procedure. This requires two inputs, the sampling time T_S between two adjacent points in the spectrum and the RC filter time constant τ_{RC}.

9. FITTING

It is the dream of every EPR practitioner to have a simulation program that is able to automatically fit an experimental EPR spectrum and return the values of SH parameters of the spin system underlying the spectrum,

including their uncertainties. Despite much effort, this is currently not possible. The many available least-squares fitting algorithms provide tools that allow the user to find a good fit only if applied properly and within their capabilities. An absolute prerequisite for a good fit is the choice of a proper simulation model (spins, SH, broadenings, etc., as discussed in the previous sections).

With a correct model in hand, the user choices for least-squares fitting boil down to a few key aspects: First, an adequate objective function needs to be chosen. Second, a good set of starting parameters and a sufficiently narrow search range need to be identified. Third, one or several least-squares optimization algorithms need to be selected.

9.1 Objective Function

An optimization algorithm tries to minimize or maximize an objective function that measures the quality of the fit between a simulated spectrum y_{sim} and an experimental spectrum y_{exp}. Typically, this is the sum of the squared deviations (ssd), $\chi^2(p_1, p_2, \ldots) = \sum \left[y_{\mathrm{exp},i} - y_{\mathrm{sim},i}(p_1, p_2, \ldots)\right]^2 / w_i^2$. The SH parameters to be varied in the fit are denoted as p_1, p_2, etc. Weights w_i can be included that depend on the noise level or user-selected range choices. Unfortunately, this objective function can have many local minima as a function of the SH parameters, e.g., when the EPR spectrum consists of many resolved hyperfine peaks. In such cases, other objective functions can have a much smoother dependence on the SH parameters and are more likely to work: the ssd of the derivatives, the integrals, the double integrals, or the Fourier transforms of the experimental and simulated spectra (Stoll, 2011). It is important to explore several of these objective functions.

9.2 Parameter Starting Point and Search Range

The second crucial choice in a least-squares fitting workflow is the choice of an appropriate starting point for the SH parameters to be fitted. Most least-squares fitting algorithms perform best if the minimum of the objective function lies in the neighborhood of the starting point. Also, it is essential to restrict the parameter search range as much as physically reasonable to help convergence. Good starting points can be obtained either from a visual analysis of the EPR spectrum (if it lends itself to that) or from literature values of comparable systems. The importance of a good starting point and an adequate limited search region in parameter space cannot be overemphasized.

9.3 Fitting Algorithm

Lastly, it is important to choose a least-squares fitting algorithm that is adequate for the problem at hand. There are a wide variety of algorithms available. They differ in many aspects: whether they are (theoretically) able to locate the global minimum or just walk to the next local minimum, whether they are deterministic or stochastic, whether they require analytical derivatives of the spectrum with respect to the SH parameters or not, and whether they can be parallelized or not.

The most popular algorithms are the downhill simplex method due to Nelder and Mead, and the Levenberg–Marquardt algorithm (Press, Teukolsky, Vetterling, & Flannery, 2002). The first one is very robust and has a reasonable chance to escape local minima, although it can be slow. It is a good default choice for exploring the parameter space. The second one is an efficient way to locate the local minimum closest to the starting point in parameter space. Other methods include the Powell method (Hanson et al., 2004), Monte Carlo methods (Kirste, 1987), simulated annealing (Hustedt, Smirnov, Laub, Cobb, & Beth, 1997), and genetic algorithms (Filipič & Štrancar, 2001).

As with the objective function, the starting point and the parameter range, it is best to explore a variety of fitting algorithms for a given problem. Often, it is useful to combine several algorithms into two-stage hybrid algorithms, where a global method is used to locate the approximate region of the global minimum, followed by a local and more efficient method that hones in on the minimum.

10. CONCLUSIONS

Simulation methods for solid-state EPR spectra are well established. Fairly general simulation programs such as EasySpin (Stoll & Schweiger, 2006) or XSophe (Griffin et al., 1999) are easily available. The broad range of paramagnetic centers gave rise to a broad range of simulation methods that are efficient for particular classes of centers. From a user perspective, it is important to be aware of the wide range of choices available to be able to identify and pick the correct combination of spin system, SH, dynamical regime, theory level, orientational and structural disorder, broadening model, and experimental distortions. Otherwise, physically unreasonable spectra are possible, and conclusions can potentially be wrong.

In contrast to the systematic workflow for setting up and performing EPR simulations, the process of using least-squares algorithms to fit a simulation to experimental data still remains a trial-and-error procedure, for which there is no silver bullet.

REFERENCES

Abragam, A., & Bleaney, B. (1986). *Electron paramagnetic resonance of transition ions*. New York: Dover.

Atherton, N. M. (1993). *Principles of electron spin resonance*. Chichester: Ellis Horwood.

Belford, G. G., Belford, R. L., & Burkhalter, J. F. (1973). Eigenfields: A practical direct calculation of resonance fields and intensities for field-swept fixed-frequency spectrometers. *Journal of Magnetic Resonance*, *11*, 251–265.

Bencini, A., & Gatteschi, D. (1990). *Electron paramagnetic resonance of exchange coupled systems*. Heidelberg: Springer.

Borrás-Almenar, J. J., Clemente-Juan, J. M., Coronado, E., & Tsukerblat, B. S. (2001). MAGPACK a package to calculate the energy levels, bulk magnetic properties, and inelastic neutron scattering spectra of high nuclearity spin clusters. *Journal of Computational Chemistry*, *22*(9), 985–991.

Chilton, N. F., Anderson, R. P., Turner, L. D., Soncini, A., & Murray, K. S. (2013). PHI: A powerful new program for the analysis of anisotropic monomeric and exchange-coupled polynuclear d- and f-block complexes. *Journal of Computational Chemistry*, *34*, 1164–1175.

Claridge, R. F. C., Tennant, W. C., & McGavin, D. G. (1997). X-band EPR of Fe^{3+}/$CaWO_4$ at 10 K: Evidence for large magnitude high spin Zeeman interactions. *Journal of Physics and Chemistry of Solids*, *58*, 813–820.

Filipič, B., & Štrancar, J. (2001). Tuning EPR spectral parameters with a genetic algorithm. *Applied Soft Computing*, *1*, 83–90.

Froncisz, W., & Hyde, J. S. (1980). Broadening by strains of lines in the g-parallel region of Cu^{2+} EPR spectra. *The Journal of Chemical Physics*, *73*, 3123–3131.

Gaffney, B. J., & Silverstone, H. J. (1998). Simulation methods for looping transitions. *Journal of Magnetic Resonance*, *134*, 57–66.

Golombek, A. P., & Hendrich, M. P. (2003). Quantitative analysis of dinuclear manganese(II) EPR spectra. *Journal of Magnetic Resonance*, *165*, 33–48.

Griffin, M., Muys, A., Noble, C., Wang, D., Eldershaw, C., Gates, K. E., et al. (1999). XSophe, a computer simulation software suite for the analysis of electron paramagnetic resonance spectra. *Molecular Physics Reports*, *26*, 60–84.

Hagen, W. R. (2007). Wide zero field interaction distributions in the high-field EPR of metalloproteins. *Molecular Physics*, *105*, 2031–2039.

Hagen, W. R., Hearshen, D. O., Sands, R. H., & Dunham, W. R. (1985). A statistical theory for powder EPR in distributed systems. *Journal of Magnetic Resonance*, *61*, 220–232.

Hanson, G. R., Gates, K. E., Noble, C. J., Griffin, M., Mitchell, A., & Benson, S. (2004). XSophe-Sophe-XeprView: A computer simulation software suite (v. 1.1.3) for the analysis of continuous wave EPR spectra. *Journal of Inorganic Biochemistry*, *98*, 903–916.

Harris, E. A., & Owen, J. (1963). Biquadratic exchange between Mn^{2+} ions in MgO. *Physical Review Letters*, *11*(1), 9–10.

Heinzer, J. (1971). Fast computation of exchange-broadened isotropic E.S.R. spectra. *Molecular Physics*, *22*(1), 167–177.

Hudson, A., & Luckhurst, G. R. (1969). The electron resonance line shapes of radicals in solution. *Chemical Reviews*, *69*(2), 191–225.

Hustedt, E. J., Smirnov, A. I., Laub, C. F., Cobb, C. E., & Beth, A. H. (1997). Molecular distances from dipolar coupled spin-labels: The global analysis of multifrequency continuous wave electron paramagnetic resonance data. *Biophysical Journal*, *74*, 1861–1877.

Hyde, J. S., Pasenkiewicz-Gierula, M., Jesmanowicz, A., & Antholine, W. E. (1990). Pseudo field modulation in EPR spectroscopy. *Applied Magnetic Resonance*, *1*, 483–496.

Iwasaki, M. (1974). Second-order perturbation treatment of the general spin Hamiltonian in an arbitrary coordinate system. *Journal of Magnetic Resonance*, *16*, 417–423.

Kirste, B. (1987). Least-squares fitting of EPR spectra by Monte Carlo methods. *Journal of Magnetic Resonance*, *73*, 213–224.

Kneubühl, F. K. (1960). Line shapes of electron paramagnetic resonance signals produced by powders, glasses, and viscous liquids. *The Journal of Chemical Physics*, *33*(4), 1074–1078.

Mabbs, F. E., & Collison, D. (1992). *Electron paramagnetic resonance of d transition metal compounds*. Amsterdam: Elsevier.

Mombourquette, M. J., Tennant, W. C., & Weil, J. A. (1986). EPR study of Fe^{3+} in α-quartz. *The Journal of Chemical Physics*, *85*(1), 68–79.

Neese, F. (2004). Zero-field splitting. In M. Kaupp, M. Bühl, & V. G. Malkin (Eds.), *Calculation of EPR and NMR parameters* (pp. 541–566). Weinheim: Wiley-VCH.

Nielsen, R. D., Hustedt, E. J., Beth, A. H., & Robinson, B. H. (2004). Formulation of Zeeman modulation as a signal filter. *Journal of Magnetic Resonance*, *170*, 345–371.

Pake, G. E., & Estle, T. L. (1973). *The physical principles of electron paramagnetic resonance*. Reading, MA: Benjamin.

Patchkovskii, S., & Schreckenbach, G. (2004). Calculation of g-tensors with density functional theory. In M. Kaupp, M. Bühl, & V. G. Malkin (Eds.), *Calculation of NMR and EPR parameters* (pp. 505–532). Weinheim: Wiley-VCH.

Pilbrow, J. R. (1990). *Transition ion electron paramagnetic resonance*. Oxford: Clarendon Press.

Piligkos, S., Weihe, H., Bill, E., Neese, F., El Mkami, H., Smith, G. M., et al. (2009). EPR spectroscopy of a family of $Cr^{III}{}_7Mn^{II}$ (M = Cd, Zn, Mn, Ni) "wheels": Studies of isostructural compounds with different spin ground states. *Chemistry - A European Journal*, *15*, 3152–3167.

Ponti, A. (1999). Simulation of magnetic resonance static powder lineshapes: A quantitative assessment of spherical codes. *Journal of Magnetic Resonance*, *138*, 288–297.

Press, W. H., Teukolsky, S. A., Vetterling, W. T., & Flannery, B. P. (2002). *Numerical recipes in C* (2nd ed.). New York: Cambridge University Press.

Robinson, B. H., Mailer, C., & Reese, A. W. (1999). Linewidth analysis of spin labels in liquids. *Journal of Magnetic Resonance*, *138*, 199–209.

Rudowicz, C., & Karbowiak, M. (2015). Disentangling intricate web of interrelated notions at the interface between the physical (crystal field) Hamiltonians and the effective (spin) Hamiltonians. *Coordination Chemistry Reviews*, *287*, 28–63.

Shaw, J. L., Wolowska, J., Collison, D., Howard, J. A. K., McInnes, E. J. L., McMaster, J., et al. (2006). Redox non-innocence of thioether macrocycles: Elucidation of the electronic structures of mononuclear complexes of gold(II) and silver(II). *Journal of the American Chemical Society*, *128*, 13827–13839.

Speldrich, M., Schilder, H., Lueken, H., & Kogerler, P. (2011). A computational framework for magnetic polyoxometalates and molecular spin structures: CONDON 2.0. *Israel Journal of Chemistry*, *51*(2), 215–227.

Stevensson, B., & Edén, M. (2006). Efficient orientational averaging by the extension of Lebedev grids via regularized octahedral symmetry expansion. *Journal of Magnetic Resonance*, *181*, 162–176.

Stoll, S. (2011). High-field EPR of bioorganic radicals. In B. C. Gilbert, D. M. Murphy, & V. Chechik (Eds.), *Vol. 22. Electron paramagnetic resonance* (pp. 107–154). Cambridge: Royal Society of Chemistry.

Stoll, S. (2014). Computational modeling and least-squares fitting of EPR spectra. In S. K. Misra (Ed.), *Multifrequency electron paramagnetic resonance* (pp. 69–138). Weinheim: Wiley-VCH.

Stoll, S., & Schweiger, A. (2003). An adaptive method for computing resonance fields for continuous-wave EPR spectra. *Chemical Physics Letters*, *380*, 464–470.

Stoll, S., & Schweiger, A. (2006). EasySpin, a comprehensive software package for spectral simulation and analysis in EPR. *Journal of Magnetic Resonance*, *178*, 42–55.

Wang, D., & Hanson, G. R. (1995). A new method for simulating randomly oriented powder spectra in magnetic resonance: The Sydney opera house (SOPHE) method. *Journal of Magnetic Resonance. Series A*, *117*, 1–8.

Weil, J. A., & Bolton, J. R. (2007). *Electron paramagnetic resonance. Elementary theory and practical applications*. Hoboken, NJ: Wiley.

Weil, J. A., Buch, T., & Clapp, J. E. (1973). Crystal point group symmetry and microscopic tensor properties in magnetic resonance spectroscopy. *Advances in Magnetic Resonance*, *6*, 183–257.

Weisser, J. T., Nilges, M. J., Sever, M. J., & Wilker, J. J. (2006). EPR investigation and spectral simulations of iron-catecholate complexes and iron-peptide models of marine adhesive cross-links. *Inorganic Chemistry*, *45*, 7736–7747.

Zalibera, M., Jalilov, A. S., Stoll, S., Guzei, I. A., Gescheidt, G., & Nelsen, S. F. (2013). Monotrimethylene-bridged Bis-p-pheneylenediamine radical cations and dications: Spin states, conformations, and dynamics. *The Journal of Physical Chemistry. A*, *117*, 1439–1448.